NUMERICAL SIMULATION OF COMBINED CO-CURRENT/COUNTER-CURRENT SPONTANEOUS IMBIBITION

Douglas W. Ruth[1], Geoffrey Mason[2], Martin A. Fernø [3], Åsmund Haugen[4]
Norman R. Morrow[2], Rasoul Arabjamaloei[1]

[1]Centre for Engineering Professional Practice and Engineering Education, University of Manitoba, Canada
[2] Department of Chemical and Petroleum Engineering, University of Wyoming, USA
[3]Department of Physics and Technology, University of Bergen, Norway
[4]Statoil , Sandslihaugen, Bergen, Norway

ABSTRACT

This paper describes a numerical study of combined co-/counter-current spontaneous imbibition of water into a core sample that is initially fully oil saturated with the two-ends-open-free (TEO-free) boundary geometry, as given by a sample with one end in contact with brine and the other in contact with oil. The present study uses an explicit simulator with an upstream differencing scheme which allows flows of the oil in both directions without blockage because of zero-saturation cells. The boundary conditions are modelled using zero-width boundary cells with fixed saturations. The saturation at the end face in contact with brine fixes the capillary bubble pressure (the pressure required to produce non-wetting fluid) at this face. All the simulations used a single set of relative permeability curves. The experimental results were matched using an automatic search technique with the capillary pressure curve as the fitting parameter. In all cases, tabular values of capillary pressure were used, with six points in the curves and linear interpolation between points. Fits were achieved using the oil productions at the two faces as the test data. It was found that all the data could be fitted using comparable capillary pressure curves. A comparison between the results obtained using the numerical simulator and a piston-like flow model published with the original experimental data provides support for the assumption of piston-like flow. The paper demonstrates both the power of numerical simulation and the urgent need for a method to either predict or accurately measure the imbibition face saturation during spontaneous imbibition.

INTRODUCTION

The problem of co-current and counter-current imbibition has attracted much recent interest in the petroleum community because these are the mechanisms whereby matrix

oil can be produced into fractures in a reservoir [1,2]. There is now a body of experimental data for short samples undergoing these processes as well as an approximate theory to explain the observed behaviour [3,4,5]. The present paper reports on a numerical-simulation study of a selection of these data. The numerical simulator is a further development of work reported previously [6,7,8,9].

The problem under consideration is shown schematically in Figure 1. A sample, originally saturated with oil, is confined radially by a sealed surface. It is then set up axially between two reservoirs, a reservoir that is filled with water and contacts the left face of the sample and a reservoir that is filled with oil and contacts the right face of the sample. The oil in the reservoir is identical to the oil that saturates the sample. It is assumed that the pressures of the fluids in the two reservoirs remain constant and equal throughout an experiment. It is assumed that the sample is strongly water-wet, and that the porosity and permeability are constant and uniformly distributed. In this configuration, it is possible for water to spontaneously imbibe into the sample, displacing oil in both a counter-current fashion (causing oil production at the left face of the sample) and a co-current fashion (causing oil production at the right face of the sample). A pressure tap is located toward the right face of the sample.
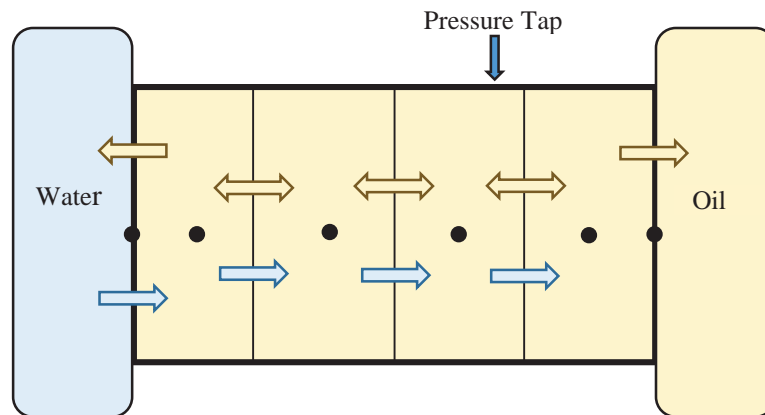
Figure 1. A schematic depiction of the problem under consideration during spontaneous imbibition with the TEO-free boundary condition.

Figure 1 shows the grid system that is used in the numerical simulation. At both ends of the sample, zero-width grid blocks are located to facilitate the definition of boundary conditions. The sample is then divided into a number of equal-width grid blocks. The simulation accounts for changes in saturation in a grid block by taking the difference between the flow rates across the boundaries. The flow rates at the boundaries are calculated using the modified-Darcy law equations. In the absence of gravity, these equations are:

$$\frac{Q_w\,\mu_w}{k\,A\,k_{rw}} = -\,\frac{dP_w}{dx} \tag{1}$$

$$\frac{Q_o\,\mu_o}{k\,A\,k_{ro}} = -\,\frac{dP_o}{dx} \tag{2}$$

$$Q_t = Q_w + Q_o \tag{3}$$

$$\frac{dP_c}{dx} = \frac{dP_o}{dx} - \frac{dP_w}{dx} \tag{4}$$

In these equations, Q is volumetric flow rate, μ is viscosity, k is permeability, A is cross-sectional area, k_r is relative permeability, P is pressure, and x is axial location. With regard to the subscripts, w denotes water, o denotes oil, t denotes total, and c denotes capillary. Equations 1 through 4 may be combined to obtain the following equation for the flow of oil:

$$Q_o = \frac{Q_t\,\mu_w\,k_{ro}}{k_{ro}\,\mu_w + k_{rw}\,\mu_o} - \frac{A\,k\,k_{ro}\,k_{rw}}{k_{ro}\,\mu_w + k_{rw}\,\mu_o}\,\frac{dP_c}{dx} \tag{5}$$

Because the simulation depends on calculating saturation changes, it follows that saturations will be known for each grid block at any time. However, this does not allow direct evaluation of Equation 5 because the total volumetric flow rate is not known *a priori* for spontaneous imbibition problems. This shortcoming can be overcome by combining Equations 2 and 5 to obtain

$$-\frac{dP_o}{dx} = \frac{Q_t}{k\,A}\frac{\mu_w\,\mu_o}{k_{ro}\,\mu_w + k_{rw}\,\mu_o} - \frac{k_{rw}\,\mu_o}{k_{ro}\,\mu_w + k_{rw}\,\mu_o}\,\frac{dP_c}{dx} \tag{6}$$

The pressures in the water reservoir at the left face of the sample and the oil reservoir at the right face of the sample are known (they have been assumed to have the same value and this value can arbitrarily be set to zero). Further, for the simulation model, if the saturation at the left face can be assumed or calculated, then the pressure in the oil at the two faces will be known. The right-hand-side of Equation 6 is a function only of saturation with Q_t being a constant value throughout the sample at any given time. Knowing the saturation profile at any time, integration of Equation 6 (in the simulator this integration is performed numerically) yields the following equation for the total volumetric flow rate:

$$Q_t = \frac{(P_{or} - P_{ol}) - \int_l^r \dfrac{k_{rw}\,\mu_o}{k_{ro}\,\mu_w + k_{rw}\,\mu_o}\,\dfrac{dP_c}{dx}}{\dfrac{1}{k\,A}\displaystyle\int_l^r \dfrac{\mu_w\,\mu_o\,dx}{(k_{ro}\,\mu_w + k_{rw}\,\mu_o)}} \tag{7}$$

Here the subscripts r and l refer to the right and left faces of the sample.
A critical feature of the simulation is the assumption for the saturation used in calculating relative permeabilities for the flows across the grid-cell boundaries. In all cases, the saturation for a fluid is assumed to be the value for the upstream cell, the so-called

"upstream-differencing" assumption. That is, if the flow rate of fluid crossing a cell boundary is left-to-right, the saturation of the left-hand cell is used. It follows that, for the case of counter-current imbibition at a grid-block boundary, the relative permeability of the water is calculated using the saturation of water in the left-hand cell while the relative permeability of the oil is calculated using the saturation of oil in the right-hand cell. The fundamental importance of this assumption can be seen by considering the left-hand sample face condition. Upstream-differencing means that the flow into the sample is controlled by the saturation of the fluid saturating the zero-volume surface cell. As this cell has zero-volume, it can instantly take on any saturation. For the present study, the saturation of the left-face is assumed to be the final average saturation of the sample. This means that there is a finite relative permeability for water to enter the sample despite the fact that the sample is fully saturated with oil. (It is noted that a theoretical determination of the value of saturation and bubble pressure (the pressure required to produce non-wetting fluid) at the left-face in spontaneous imbibition problems is the most important unresolved issue for the problem of spontaneous imbibition.)

THE PROGRAM OF STUDY

For the present study, three previously published data sets [3,4] were considered. As can be seen in Table 1, these tests used samples with similar petrophysical properties, the same water, but oils with a wide range of viscosities.

Table 1   The petrophysical characteristics of the three samples under study.

Sample	ϕ	L (cm)	D (cm)	Tap (cm)	ρ_w (kg/m^3)	μ_w (cp)	ρ_o (kg/m^3)	μ_o (cp)	K (md)
CHP07	0.467	14.25	3.79	11.25	1005	1.09	740	1.47	5.50
CHP11	0.466	6.10	3.81	3.23	1005	1.09	870	137.0	4.40
CHP25	0.458	5.75	3.70	3.43	1005	1.09	840	83.3	4.08

The published results [3,4] report the range for the permeability to be 3 to 6 mD. For the purpose of simulation, more accurate values are needed. These values were determined by examining the early-time data (before a front could pass the pressure tap) for the pressure and right-face production rates. This calculation is illustrated in Figure 2 for Sample CHP07; the permeabilities calculated in this manner are shown in Table 1.

The history matches were achieved by using a single set of relative permeability curves and modifying the capillary pressure curve. Pressure behavior is more complex than production; the errors between the experimental and simulated results were based on the productions at the each face of the samples. Comparison of the predicted and the experimental pressures provides an independent test of the quality of the analysis.
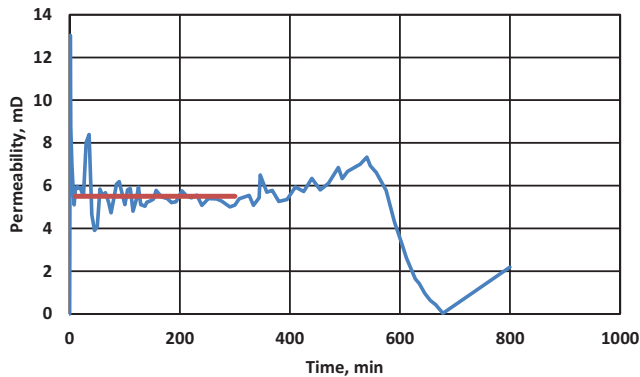
Figure 2. The calculated permeability for Sample CHP07 showing the range of times (the red line) used to determine the mean permeability.

The simulations used the relative permeabilities reported by [3]. These curves are shown in Figure 3. The history-matching process was straightforward. The capillary pressures were input as a 6-entry table. For the search, various stages of keeping the saturations constant and varying the capillary pressures, and *vice versa* were employed. For each assumed capillary pressure curve, a simulation was run and the errors between the simulated productions and the values calculated from experimental data were computed. By using an exhaustive search technique, the capillary pressure curve that led to the minimum error was determined.
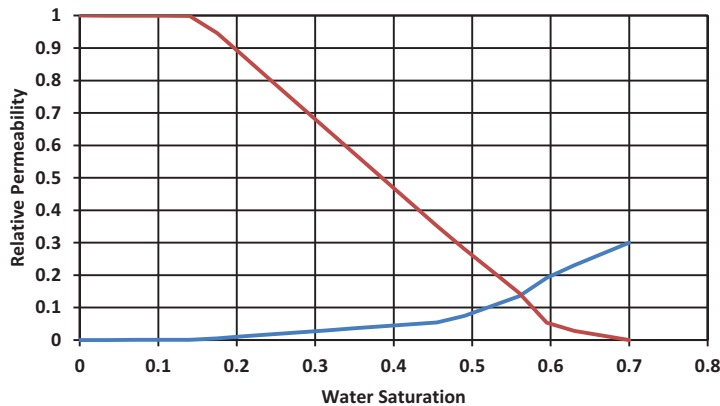
Figure 3. The relative permeability curves used in the simulations.

All simulations were run using a total of 50 grid blocks. Stability was controlled by limiting saturation changes in any one grid block to less than 0.0001. No stability problems were encountered and each test simulation ran in under 20 seconds.

RESULTS

Figure 4 shows the capillary pressure curves that lead to the best fits for the three samples. Also shown is the initial "guess" for the capillary curve which was based on the

data from [3]. All three simulation curves show similar shapes and magnitudes and do not greatly differ from the initial curve. It is noted that the small negative region at high water saturation are not physically reasonable for a strongly water-wet sample. They were included here because they were present in the original "initial" curve. In all cases, the simulations predicted capillary pressures in the positive region and water saturations never exceeded the zero-capillary pressure saturation. The shapes of these curves may appear to be unusual; however, it must be recalled that the region from $0 < S_w < 0.3$ does not actually occur in the tests and these values are really an artifact of the fitting technique.

The quality of the curve fits for the three samples can be seen in Figures 5 through 7. In all cases, agreement between the predicted and measured productions is very good. Of special interest is the remarkable agreement between the predicted and measured pressures. Recall that these data were not used in the history matches. In Figure 5, the spike in pressure after 600 minutes is clearly matched. For both Figures 6 and 7 the bi-modal nature of the pressure behavior is captured although agreement between the two data sets is not nearly as good as that demonstrated in Figure 5.
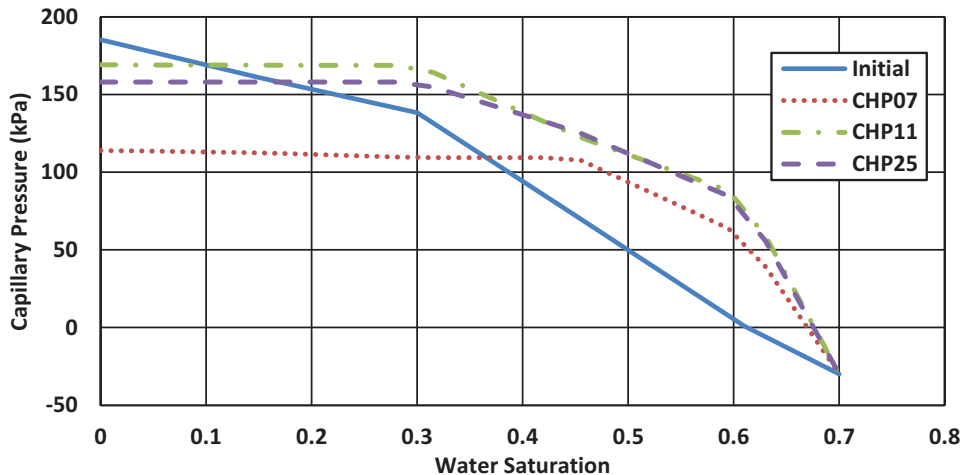
Figure 4. The capillary pressure curves that lead to the best fits of the experimental data. Also shown is the capillary curve from [3] (labelled "Initial").

In the case of Sample CHP07 (Figure 5), μ_o/μ_w equal to 1.35, production from the left hand face is minimal. The simulation was very successful in predicting both the small counter-current left-face production and the more substantial co-current right-face production. Production at the right-face became very slow near the end of the experiment; this feature was also captured by the simulator. This slowing of production corresponds to the arrival of water at the right-face. The pressure history of the experiment is quite complex with a sharp drop at early times, then a relatively gradual linear decline followed by a sharp peak just before the end of the imbibition process.. All of these features are predicted by the simulator. It must be emphasized that pressure was not used during the history-match. The agreement between experiment and simulation

provides confidence in the simulation. Note that for Sample CH07, production dropped off quickly after the water first arrived at the right face.
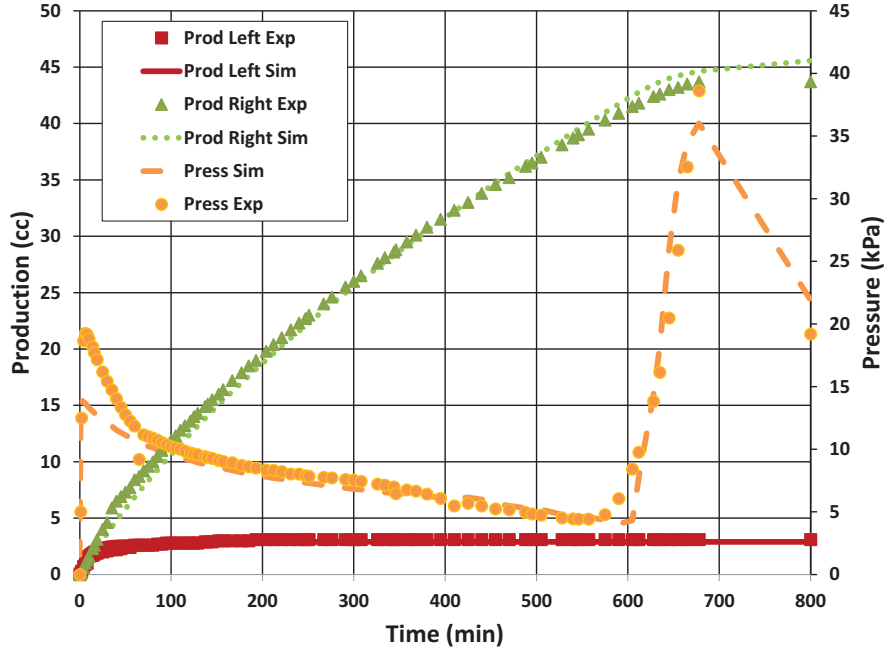
Figure 5. A comparison of experimental and simulated results for sample CHP07. Predominantly co-current oil production with a viscosity ratio (μ_o/μ_w) equal to 1.35.

In the case of Sample CHP11 (Figure 6), μ_o/μ_w equal to 125, production at the left-face is more substantial. Again the simulation captures the relative productions very well. Unlike the low viscosity ratio case (Sample CHP07) the production at the right end of the sample continues after about 600 minutes, although at a lower rate. This point roughly corresponds to a local minimum in the pressure – it also corresponds to the time the water first reaches the right-face of the sample. Although not a perfect match, the simulated pressure history shows all the features of the experimental curve: an initial rise, a drop to a local minimum, a second rise and an eventual tailing off. A significant difference between these results and the results for the low viscosity ratio case is that oil production at the right face continued, albeit at a reduced rate, after the arrival of water at this face.

In the case of Sample CHP25 (Figure 7), μ_o/μ_w equal to 76, all the main features of Sample CHP11 are demonstrated. The simulation does not match the experimental results as well as in the first two cases but the agreement is still very good.
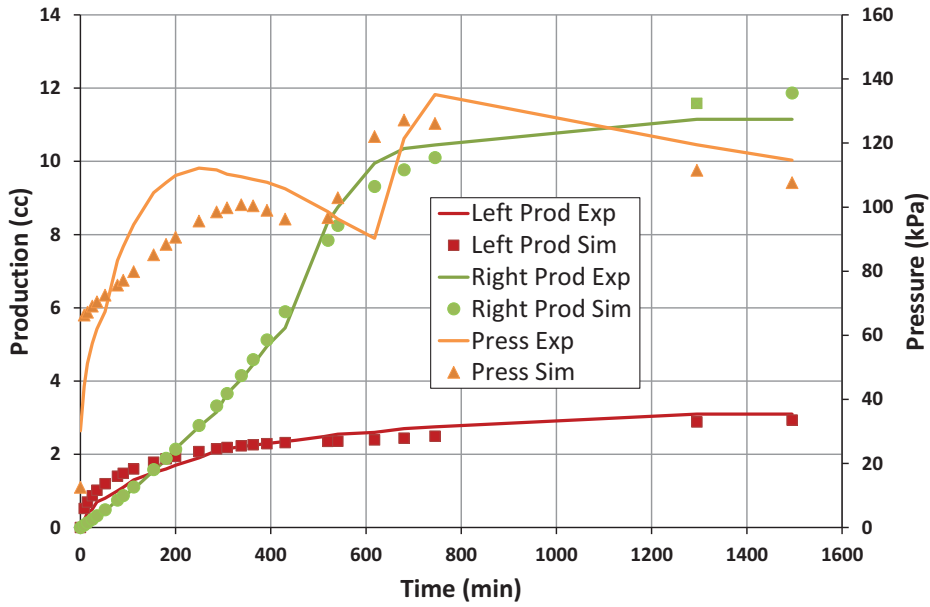
Figure 6.   Results for sample CHP11. Sustained counter-current imbibition, but still predominantly co-current oil production with a viscosity ratio (μ_o/μ_w) equal to 125.
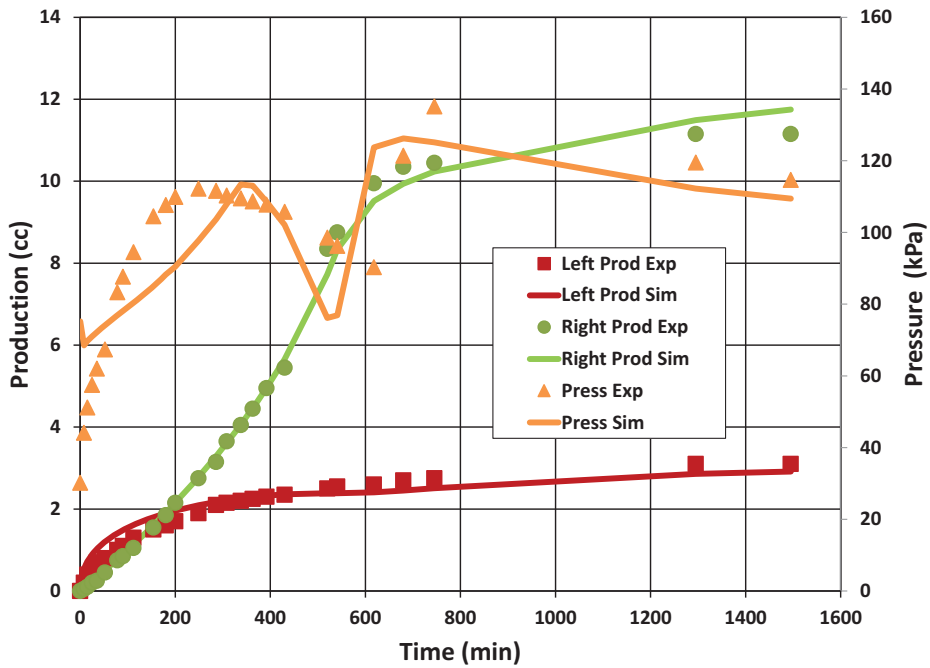
Figure 7.   Results for sample CHP25. Sustained counter-current imbibition, but still predominantly co-current oil production with a viscosity ratio (μ_o/μ_w) equal to 76.

Comparison with Piston-Like Flow Theory
Figure 8 shows the calculated saturation profiles for Sample CHP25. A model which assumes piston-like flow has been published for both counter- and co-current imbibition [4]. This figure clearly shows that displacement takes place in an essentially frontal manner (tied to the low-to-zero permeability to brine for $S_w < 0.3$). However, with a wedge-shaped region extending from the imbibition face to the front, this is a clear departure from the piston model. However, the maintained similarity of the profiles is consistent with the close match to experimental results given by a piston-like flow model.
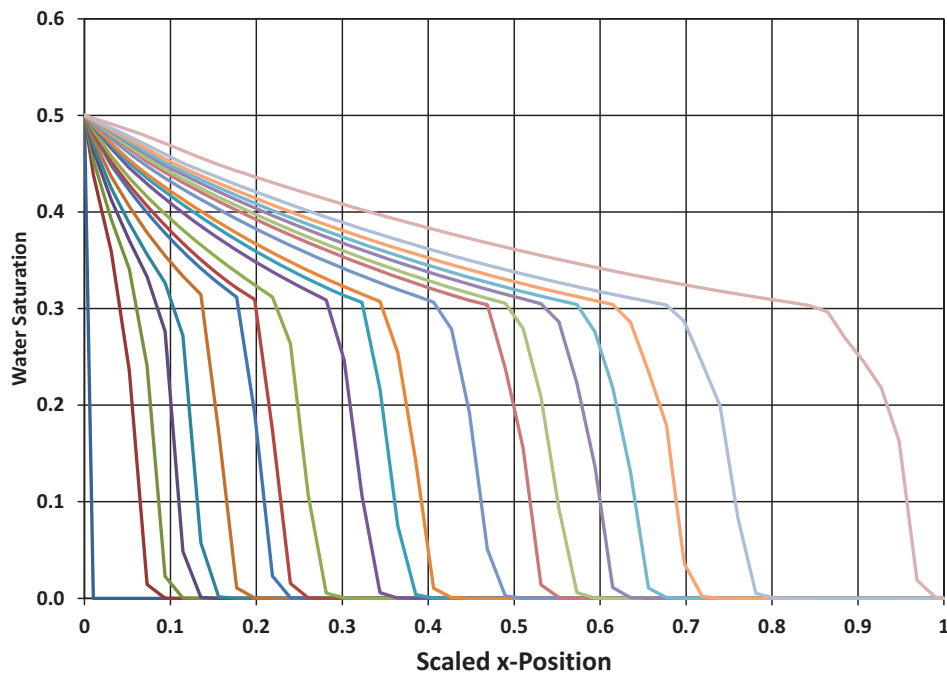
Figure 8. Water saturation profiles for CHP25.

Further comparisons between the results of the present study and the piston-like flow model are given in Table 2. These results show various levels of agreement. The permeability results differ because the present paper uses a different averaging procedure. However, these results are very similar. For the piston-like flow, the front is perfectly defined. However, in the simulations, fronts are generally smeared and a single saturation is hard to quantify. The capillary pressures at the front and at the inlet show reasonable agreement. The results for the relative permeabilities at the front do not show particularly good agreement. However, it must be noted that the simulation used a set of input curves based on independent experiments while the piston-like flow uses a single point calculation. In light of this, the agreement between the results for $k_{w,f}$ in Samples CHP11 and CHP25 is satisfactory.

Figure 9 gives a visual depiction of the agreement between the capillary pressure curves determined through simulation and the frontal saturation/capillary pressure points predicted by the piston-like flow theory. The piston-like flow theory is based on a single saturation point but the points for the two samples with published data agree very well with the points on the capillary pressure curves found by history matching with the simulator.

Table 2 A comparison between the results obtained by simulation and results obtained using piston-type flow theory.

Property	k (md)	$P_{c,o}$ (kPa)	$S_{w,f}$	$P_{c,f}$ (kPa)	$k_{w,f}$	$k_{nw,f}$
CHP07: Simulation	5.6	85	0.48	96	0.07	0.28
CHP07: Piston-like flow	5.0	34	NA	78	0.2	na
CHP11: Simulation	4.49	55	0.38	127	0.2	0.56
CHP11: Piston-like flow	4.58	80	0.45	128	na	0.77
CHP25: Simulation	4.08	117	0.31	166	0.023	0.64
CHP25: Piston-like flow	4.83	80	0.45	118	na	0.51
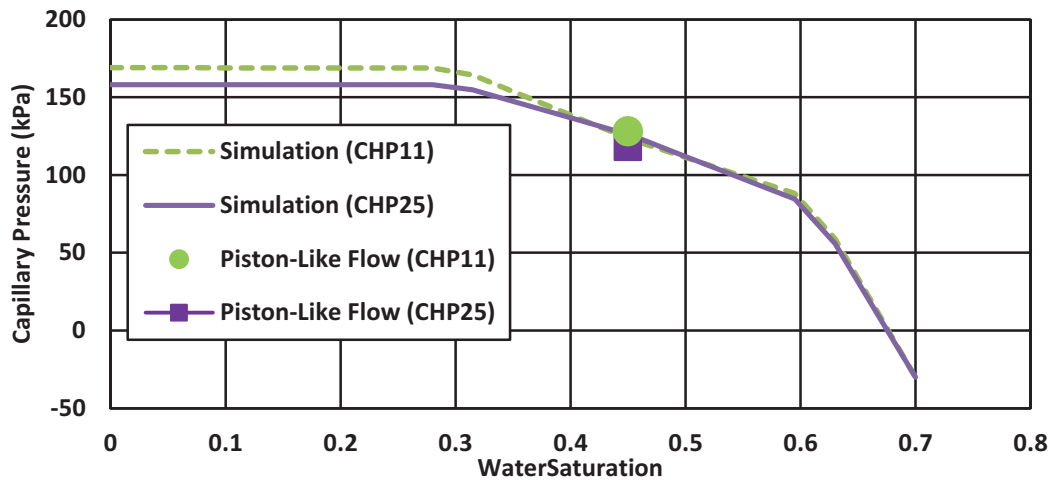
Figure 9. Comparison of Piston-like flow and Simulation Results.

Overall, the simulations support the conclusion that the piston-like flow gives a very good first estimate of the saturation functions.

DISCUSSION
Despite the very good history matches obtained in the present study, there are a number of issues that need further attention. The most important issue is that the present study uses relative permeability curves obtained in an independent experiment. The results therefore are founded on the assumption that the relative permeability curves are unique functions of the sample, not of the process. A related concern is that the relative

permeabilities obtained in the present study vary considerably from those obtained by the piston-like flow theory. Another important issue is that the saturation at the inlet face of the sample was simply set to the final average saturation of the sample. A method to theoretically predict this saturation, and its detailed physical significance, in a unique manner does not yet exist. A third issue is that experimental saturation profiles are not available for the comparisons in the present work. New, related imbibition results, with imaging of the advancing imbibing front, are now available [10]   Close observation (not detailed above) of the various test values used in obtaining the best history matches shows that significantly different capillary pressure curves can lead to quite comparable levels of error.   Until simulations that include production/pressure/saturation profile information are available, based on results such as those presented in [10], results from modeling this problem must be used with caution.

CONCLUSIONS
The following conclusions can be made based on the present study:
1. The results of three water-oil, combined counter- and co-current experiments, using a range of oil-viscosities, were successfully matched using a single set of relative permeability curves. The resulting, fitted capillary pressure curves were very comparable in both shape and magnitude.
2. The results of the simulations were largely consistent with the previously published results produced using a piston-like flow theory (see [4]).
3. Because of its complex behavior, the TEO-free boundary condition offers opportunities for evaluation several core/fluid properties from a single experiment. If a range of fluid viscosity is used then it is possible that more variables can be inferred [11].

ACKNOWLEGEMENTS

REFERENCES

1. Mason, G. and N.R. Morrow, "Recovery of Oil by Spontaneous Imbibition", *Current Opinions in Colloid Interface Science*, (2001), Vol.6, pp.321-337.
2. Mason, G. and N.R. Morrow, "Developments in Spontaneous Imbibition and Possible Future Work", *Journal of Petroleum Science and Engineering*, (2013).
3. Haugen, Å., M.A. Fernø, G. Mason, N.R. Morrow, "The Effect of Viscosity on Relative Permeabilities Derived from Spontaneous Imbibition Tests", *Transport in Porous Media,*(2015), Vol.106, pp.383-404.
4. Haugen, Å., M.A. Fernø, G. Mason, N.R. Morrow, "Capillary Pressure and Relative Permeability Estimated from a Single Spontaneous Imbibition Test", *Journal of Petroleum Science and Engineering*, (2014), Vol.115, pp.66-77.
5. Fernø, M.A., Å, Haugen, G. Mason, N.R. Morrow, "Measurement of Core Properties Using a New Technique – Two Ends Open Spontaneous Imbibition", SCA2014-006, *International Symposium of the Society of Core Analysts*, (2014), Avignon, France, 8-11 September.
6. Ruth, D.W., G. Mason, N.R. Morrow, "A Numerical Study of the Influence of Sample Shape on Spontaneous Imbibition", SCA2003-016, *International Symposium of the Society of Core Analysts*, (2006), Pau, France, 21-24 September.
7. Ruth, D.W., N.R. Morrow, Y. Li, J.S. Buckley, "A Simulation Study of Spontaneous Imbibition", SCA2000-024, *International Symposium of the Society of Core Analysts*, (2000), Abu Dhabi, UAE, 18-22 October.
8. Ruth, D.W., G. Mason, N.R. Morrow, Y. Li, "The Effect of Fluid Viscosities on Counter-Current Spontaneous Imbibition", SCA2004-011, *International Symposium of the Society of Core Analysts*, (2004), Abu Dhabi, UAE, 5-9 October.
9. Li, Y., D.W. Ruth, G. Mason, N.R. Morrow, "Pressures Acting in Counter-Current Spontaneous Imbibition", Journal of Petroleum Science and Engineering, (2006), Vol.52, No.1-4, pp.87-99.
10. Fernø, M.A., Haugen Å., Brattekås, B., Mason, G. and Morrow, N.R. "Quick and Affordable SCAL: Spontaneous Core Analysis. SCA2015-A055, *International Symposium of the Society of Core Analysts*, (2015), St. John's, Canada, 16-21 August.
11. Meng, Q., H. Liu, and J.Wang, "Entrapment of the Non-wetting Phase during Co-current Spontaneous Imbibition" *Energy & Fuels*, 2015. 29(2): p. 686-694.